Life in Silico (2024) 2(1), 1-16

LIFE IN SILICO
https://life-insilico.com

RESEARCH ARTICLE

OPEN ACCESS

Detailed quantum chemical, ADMET, reactivity, and molecular docking interaction analysis of potential phytochemicals from *Asparagus racemosus* targeting HIV enzyme/DNA receptors

Meenakshi Rana[a*], Shradha Lakhera[a], Kamal Devlal[a]

[a] *Uttarakhand Open University, School of Sciences, Department of Physics, Haldwani, 263139, Uttarakhand, India*

ARTICLE INFO

Article History:

Received: 10 September 2023
Revised: 14 December 2023
Accepted: 14 December 2023
Available online: 28 December 2023

Edited by: E. S. Istifli

Keywords:

Molecular docking
In silico
DFT
Asparagus
Human immunodeficiency virus

ABSTRACT

Acquired immune deficiency syndrome is a life-threatening disease that is still uncured and takes the lives of thousands of people every year. Along with medical aids, herbal extracts, and natural products have parallel importance in inhibiting diseases. The present study aims to discover the potential phytochemicals of *Asparagus racemosus* that can inhibit HIV-AIDS. Ten different proteins of HIV-AIDS were considered and target macromolecules were prepared from these protein structures. A multi-stage in silico study was performed for fifteen phytochemicals of the target plant to check which phytochemical has the best inhibiting activity against the HIV-AIDS proteins. The chemical reactivity was analyzed by the reactivity parameters. All the physiochemical, drug-like, and ADMET properties of the phytochemicals were monitored. The analysis reveals that diosgenin and sarsasapogenin have the best drug-like nature among the other phytochemicals. Further, the post-docking analysis reveals that diosgenin exhibited a remarkable binding profile with all the target macromolecules of HIV-AIDS. In conclusion, the present study clarifies the potential character of diosgenin and sarsasapogenin as an inhibitor of the AIDS virus and chemical testing can be executed with the computational findings based on the proposed study.

1. Introduction

The discovery of strong inhibitors against human immune deficiency virus-acquired immune deficiency syndrome (HIV-AIDS) represents a major advancement in AIDS research showing potential antiretroviral effects in advanced medicinal clinical trials (Gillespie et al., 2019; Weiss, 2008; Zhibin et al., 2015). Despite numerous studies and the introduction of many inhibitors, HIV is still a major concern and threat to human society. The global HIV and AIDS statistics 2021 issued by United Nations AIDS reported 38.4 million people were infected by HIV and also 1.5 million people globally became freshly infected by the virus (Tabe et al., 2015). Additionally, 650.000 people died globally due to HIV infections. Different antiretroviral therapy has been used by doctors for treating HIV-AIDS (Pappas, 2013). Some of the drugs issued by the U.S. Department of Health and Human Services (HHS) and U.S. Food and Drug Administration (FDA) are Cimduo, Truvada, Descovy, Complera, Dovato, Odefsy, Stribid, Genvoya, Atripla and Symfi (Pastuch-Gawołek et al., 2019; Walsh et al., 2023). Along with the discovery of new medicines for treating HIV, the research industry has been also conducting research on the discovery of potential natural inhibitors derived from natural sources (Baker et al., 2007).

Asparagus racemosus is a native plant of the African and Asian subcontinent that have spiky leaf and red round cherry-like fruit (Joshi, 2016). This plant belongs to the Asparagaceae family. Its

Reviewed by:
Alan Carrasco-Carballo: Benemérita Universidad Autónoma de Puebla, Puebla, Mexico
Triana Kusumaningsih: Sebelas Maret University, Surakarta, Indonesia

* Corresponding author(s):
E-mail address: mrana@uou.ac.in (M. Rana)
e-ISSN: 2980-4027
doi:

common name is Shatavari and it belongs to the Plantae kingdom and angiosperm division. While *Asparagus* is its genus, racemosus is the species epithet. Its class is Monocots and its order is Asparagales (Thakur et al., 2021). There are numerous studies performed on this plant in the past. Studies carried out previously indicated that different parts of the *A. racemosus* have been influential in combatting many deadly diseases like the progression of breast carcinoma, COVID-19, estrogen receptor α, Alzheimer's disease, and many more (Bharadvaja, 2023; Majumdar et al., 2021). *A. racemosus* is an Indian plant originating in the Himalayan region of Uttarakhand state. This plant has numerous medicinal values and has been used since the historic times. Different parts of plants show antioxidant and antibacterial activities. The roots of this plant were used to increase sperm count in males and improve lactation in females (Thakur et al., 2021).

Previously, there have been many studies done in the past that account for the quantum chemical analysis, ADMET, reactivity, and molecular docking interactions of the active phytochemicals of the *A. racemosus*. Alok and the co-authors have reported a review on the phytochemistry of the phytochemicals of *A. racemosus* (Alok et al., 2013). Thirty-one different kinds of pharmacological activities have been discussed in the article including the galactagogue effect, antibacterial, antiprotozoal, gastrointestinal, antihepatotoxic, cardiovascular, immunomodulatory, antioxidant, etc. (Alok et al., 2013). An in silico study performed by Chikhale et al. (2021) reported the strong antiviral activity of the asparoside-C and asparoside-F phytochemicals against COVID-19. The binding affinity of the active phytochemicals of *A. racemosus* against macromolecules of COVID-19 obtained from molecular docking was obtained between -5 to -7 kcal/mol (Chikhale et al., 2021). A similar kind of study was reported by Sharma and Jaitak (2020) in which the investigations were done for the potential inhibition of estrogen receptor α. Estrogen receptor α is the leading macromolecule that supports the growth of breast cancer in women (Sharma & Jaitak, 2020). In this context, the roots of the *A. racemosus* have a revolutionary phytochemical, namely rutin, that exhibit remarkable binding strength with estrogen receptor α (Sharma & Jaitak, 2020). The binding affinity in the molecular docking of the rutin with estrogen receptor α was obtained as -13.7 kcal/mol which was the highest among all the other reported phytochemicals of *A. racemosus* (Sharma & Jaitak, 2020). One study was found in which the inhibiting characteristics of the phytochemicals of *A. racemosus* against different transmitting macromolecules like Erβ and ERα ligand binding domain, human placental estrone sulphatases, human 17β-hydroxysteroid dehydrogenase type 1, human glucose 6-phosphate dehydrogenase, and tubulin protein (Singla & Jaitak, 2015). These macromolecules lead to the inhibition of breast cancer progression in humans.

The present study accounts for the investigation of the inhibitory property of phytochemicals of *A. racemosus* against HIV macromolecules. A multi-stage in silico study was performed as shown in Figure 1. The molecular docking was performed for all the phytochemicals with all the target macromolecules to check the binding of the ligand at the binding sites of the receptors. The phytoconstituents with the best binding affinity were selected and the further chemical reactivity and druggability of the inhibitors were analyzed. The density functional theory (DFT) calculations were employed to express the chemical reactivity of these phytochemicals. Further, the drug-like properties and ADMET properties of all the selected phytochemicals were analyzed. The toxicity of the selected phytochemicals for the heart was accounted for using cardiotoxicity maps. The post-docking analysis was done with these five phytochemicals to check which phytochemical has the best inhibitory binding potential against the HIV macromolecules.

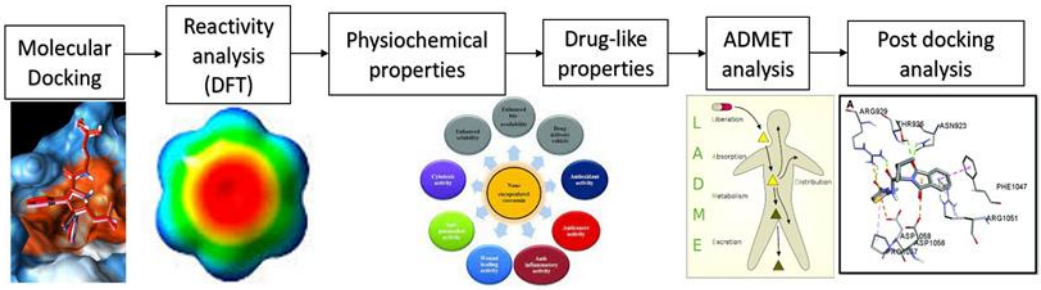

Figure 1. Herein, reported multi-stage in silico study

2. Materials and methods

2.1. Protein retrieval

All the target protein macromolecules were obtained from the online database Protein Data Bank (https://www.rcsb.org/) in .pdb file format (see supplementary file SD 1). The downloaded structures were then further processed for docking. Biovia Discovery Studio Visualizer (https://discover.3ds.com/discovery-studio-visualizer-download) was used for the primary removal of the heteroatoms from the protein structures. After heteroatom removal, the AutoDock Tools 1.5.6 (https://autodock.scripps.edu/) were used for further protein preparation. The water molecules were removed, then Kollman charges were added to the respective macromolecules (Lakhera et al., 2021). To obtain correct polarity, polar hydrogens were added, and the binding sites of the macromolecules were located (Lakhera et al., 2022a). The prepared protein macromolecules were converted into .pdbqt format for molecular docking. Ten different proteins were considered in this study. Each one was responsible for monitoring and controlling different activities of the virus. 1MM8 supports the use of Tn5 as a surrogate model for the development of HIV-1 IN inhibitors (Savarino, 2007). Tn5 is an enzyme that is responsible for the integration of the DNA fragment into genomic DNA (Delelis et al., 2008). Macromolecule 1N8X is the stem-loop RNA structure of the binding site of HIV that acts as a key to dimerization (Sun et al., 2007). Macromolecule 1RPV is responsible for regulating protein expression (Kohn & Clifford, 2002). The protein 1RZJ is HIV-1 glycoprotein 120 complexed with neutralizing antibody 17B that helps in determining the viral tropism by binding to target-cell receptors (Wang et al., 2016). There are some proteins that not only mediate HIV infection in humans but also give rise to some diseases such as tuberculosis which is most common in patients of HIV/macromolecules such as 1TVR and 1UWB that are HIV-1 RT/9-

CL TIBO and TYR 181 CYS HIV-1 RT/8-CL TIBO transmitter that support the birth and growth of TB among AIDS patients, respectively (Wang et al., 2005; Wang et al., 2001). The protein 3DIK is the structure of the HIV-1 CA pseudo-atomic model of the HIV-1 capsid protein in a hexameric lattice that is responsible for protein replication at both the early and late stages of HIV-1 (Kohn & Clifford, 2002). 4P6A is the crystal structure of a potential anti-HIV in complex with alpha-1,2-mannotriose (Wang et al., 2016). The protein 5TYR is a wild-type macromolecule that has zero drug resistance (Wang et al., 2005). The wild-type HIV macromolecule is the protein that grows in the body in the initial stages of the infection. The macromolecular structure of South African HIV-1 subtype C protease comprised with a D25A mutation with PDB ID 6I45 was also considered as a target macromolecule (Wang et al., 2001). All these protein structures were identified as the target macromolecules of HIV-AIDS in the literature.

2.2. Ligand retrieval

The phytoconstituents of the plant of interest (*A. racemosus*) were identified from the online accessible database of the natural product activity and phytochemical source "Indian Medicinal Plants, Phytochemistry and Therapeutics" (IMPPAT) (https://cb.imsc.res.in/imppat/) and the remaining ligands in PDB format were further obtained from the PubChem database (https://pubchem.ncbi.nlm.nih.gov/). A total of sixteen phytochemicals were identified and their PubChem details have been listed in supplementary file SD 2. The literature evidenced the composition and location of different phytochemicals of *A. racemosus* and the source part of the phytochemicals are illustrated in Figure 2.

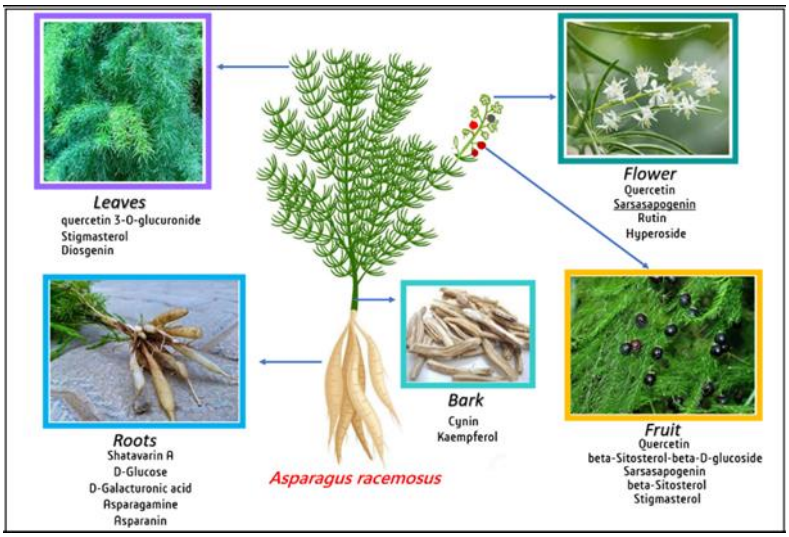

Figure 2. Morphology of the plant with phytoconstituents

2.3. Molecular docking

After the in silico preparation of the ligand and proteins, molecular docking was performed for all the phytochemicals against all the target macromolecules to determine the binding affinity of the ligands' interactions within the target macromolecules. AutoDock Tools 1.5.6 (https://autodock.scripps.edu/) were used for performing molecular docking. Different grid parameters were set for different protein structures and are mentioned in supplementary file SD 3. In AutoDock Vina, a total of 9 docking runs were performed for each ligand with the relevant protein receptor, and from these bound ligand conformations, the top-ranked pose was determined as the ligand pose showing the best binding strength with the most negative binding free energy (ΔG: kcal/mol). The docked complexes showed the highest binding affinity, low inhibition constant, high number of H bonds and hydrophobic contacts, and low drieding energy (Du et al., 2011; Ismaya et al., 2020). The post-docking analysis was then performed for the selected phytochemicals with the best binding affinities.

2.4. Density functional theory analysis

DFT tools were used for the structural optimization of the selected phytochemicals with the best binding scores. B3LYP/6-311++G(d,p) functional is the best-known and sufficient function for calculating the features of organic systems. So, the aforementioned basis set was used for structural optimization in the present study. The chemical reactivity descriptors were used for quantitatively evaluating the chemical reactivity of the phytochemicals. The energies of the highest occupied and lowest unoccupied molecular orbitals (HOMO-LUMO) were used for the calculations of reactivity descriptors (Chen et al., 2015). Koopman's identities were also used for the calculations of the reactivity descriptors (Lakhera et al., 2023a; Sherry et al., 2022).

2.5. Physiochemical properties

Physiochemical properties of the drug-like molecules reveal the physiochemical conditions of the molecules such as molecular weight, log P, topological polar surface area (TPSA), hydrogen donor and acceptors, heteroatoms, hybridization, etc (Lakhera et al., 2022b). These properties tell us whether the compounds could be stable and suitable for pharmacokinetic applications or not. LogP values give a quantitative evaluation of how well a drug will be absorbed, transported, and distributed in the body (Sherry et al., 2021). These values also indicate the formulation and dose of the compound that should be taken into account. TPSA is the extent to which the drug-like molecule shows a surface for absorption (Lakhera et al., 2022b). Heteroatoms are the structures or groups of atoms that are bonded to the molecular structure of ligands and that get bonded to the binding sites of the target macromolecules during docking and give false positive docking scores rather unstable

protein-ligand complex (Lakhera et al., 2023b). The hybridization of the ligands reveals the number of carbon atoms involved in the hybridization of the molecules (Remko et al., 2006). These properties help in getting an idea about the kinetic properties of the drug-like molecules.

2.6. Drug-likeness analysis

Drug-likeness properties are the specific features used to report the drug-like behavior of the compounds. These properties consist of the Lipinski Rule of 5, Ghose Rule, Veber's Rule, Egan's Rule, Mugge's Rule, etc. These properties tell us whether the target compound can be used as drug-like or not. The canonical molecular-input line-entry system (SMILES) of the phytochemicals from *A. racemosus* was submitted to the SwissADME (http://www.swissadme.ch/) to get the drug-like properties of the phytochemicals.

2.7. ADMET analysis

The absorption, distribution, metabolism, excretion, and toxicity (ADMET) of the drug-like compounds were monitored and explained using ADMET properties. These properties consist of bioavailability score, solubility, blood-brain-barrier penetration, gastrointestinal absorption, availability of PAINS, CYP inhibitors, and p-glycoprotein substrates. The molecules with a bioavailability score > 0.10 indicate sufficiently absorbable molecules orally (Waring, 2010). Blood-brain-barrier concentration reveals the active molecules with advanced capability to penetrate nerves present in the brain (Remko et al., 2011). Gastrointestinal absorption is the absorptive property of molecules that reveals the absorption and activity of molecules in intestinal processes (Wang et al., 2020). PAINS are the atomic groups (like heteroatoms in proteins) that can bind to the binding sites of the proteins and can give false positive values of the binding affinity during docking (Baev, 2012). The availability of these groups can give rise to false positive results while docking. The fewer the number of PAINS in ligands, the more the chances of getting true and high binding affinity (Veber et al., 2002). The potential CYP inhibitors form a stable complex with the protein's active site by binding tightly, resulting in a prolonged inactivation of the enzyme, thereby increased half-life of the drug-like compound in question. This inhibitory potential of the investigated ligand against the CYP subtypes could contribute to the sustained stability of the docked complex and lead to an increased pharmacodynamic activity (Agrawal et al., 2017).

2.8. Cardiotoxicity analysis

Canonical smiles of all the phytochemicals were used for getting the cardiotoxicity map. Pred-hERG (http://predherg.labmol.com.br/) database was used to obtain the cardiotoxicity map. Pred-hERG gives a unique probability map corresponding to each molecular smiley. This map consists of the green and pink colored counter lines over the molecular geometry in which the green regions indicate the regions with a negative contribution to hERG blockage and the pink colored regions are the higher positive contributors to hERG blockage (Varma et al., 2005). In addition to this, cardiotoxicity percent is also calculated by pred-hERG to show the extent of the molecule that imparts in the cardiotoxicity (Hosen et al., 2023). The applicability domain was also measured by pred-hERG with a limit value of 0.26 (Gorgulla et al., 2020). The ligands with applicability domain values much lower than 0.26 are known to prevent cardiotoxicity.

3. Results and discussion

3.1. Molecular docking

Molecular docking was performed for all the considered ligands of Asparagus racemosus with different proteins of HIV-AIDS. The obtained docking scores were mentioned in Table 1. All the phytoconstituents of *A. racemosus* gave good binding affinity with all the protein macromolecules of HIV. Asparanin, diosgenin, quercetin 3-*O*-glucuronide, sarsasapogenin, and shatavarin A were the phytochemicals showing the best binding affinity scores for all the proteins. Considering all the proteins, asparanin exhibits a docking score > -9 kcal/mol, with the highest scores observed for 1N8X and 1RPV. Diosgenin has a docking score > -8 kcal/mol with the highest for 1RZJ and 5DIK. Sarsasapogenin and shatavarin A have binding affinity scores of > -8 kcal/mol for all the proteins. Apart from these phytochemicals, the other phytochemicals have low binding affinity with the proteins.

Table 1. Molecular docking scores (kcal/mol) of all the phytochemicals with target proteins

Property	1MM8	1N8X	1RPV	1RZJ	1TVR	1UWB	3DIK	4P6A	5TYR	6I45
Asparagamine A	-8.5	-9.3	-5.8	-7.7	-7.9	-8.8	-8.3	-7.9	-6.9	-6.9
Asparanin	-11.0	-11.5	-11.4	-9.3	-10.7	-9.6	-10.5	-8.5	-9.0	-9.0
β-sitosterol	-7.7	-7.6	-7.6	-7.8	-8.2	-7.2	-8.4	-7.3	-6.6	-6.7
β-Sitosterol-β-D-glucoside	-8.7	-9.1	-6.2	-8.3	-8.4	-8.8	-9.3	-7.3	-7.0	-7.0
Cynin	-9.7	-10.1	-5.3	-8.8	-8.1	-7.7	-9.2	-7.6	-6.5	-6.6
D-Galacturonic acid	-6.8	-6.1	-3.8	-5.6	-6.8	-6.5	-6.4	-5.1	-5.0	-5.0
D-Glucose	-6.3	-6.1	-3.8	-5.4	-6.0	-6.3	-5.8	-4.6	-4.7	-4.7
Diosgenin	-9.7	-10.1	-6.3	-10.5	-9.5	-8.7	-10.4	-8.3	-8.8	-8.8
Hyperoside	-9.2	-9.0	-4.9	-7.8	-8.0	-7.4	-9.6	-6.9	-6.3	-6.4
Kaempferol	-8.1	-7.9	-5.3	-7.3	-8.3	-8.0	-9.2	-6.4	-6.8	-6.8
Quercetin	-8.5	-8.2	-5.2	-7.3	-8.6	-8.5	-9.4	-6.6	-6.6	-7.0
Quercetin 3-*O*-glucuronide	-9.0	-9.3	-5.1	-7.8	-8.0	-8.0	-10.4	-7.2	-6.6	-6.6
Rutin	-10.5	-10.5	-5.6	-8.9	-8.6	-7.8	-9.7	-7.5	-6.8	-6.8
Sarsasapogenin	-9.4	-10.0	-6.2	-9.5	-9.4	-8.7	-10.0	-8.1	-8.0	-8.0
Shatavarin A	-9.1	-11.1	-5.0	-8.1	-9.7	-9.4	-10.1	-7.8	-7.2	-8.0
Stigmasterol	-8.1	-8.2	-5.3	-8.2	-8.1	-7.8	-8.6	-7.6	-7.3	-7.2

3.2. Density functional theory analysis

The DFT calculations were done to verify the chemical reactivity of the selected drug-like molecules (Orr et al., 2012). Drug-like candidates must have high chemical reactivity to be drug-like (Lakhera et al., 2023c). The calculated global reactivity descriptors for the selected phytochemicals have been mentioned in Table 2. The difference between the energies of the HOMO and LUMO was considered as the band gap of the compound. The band gap of asparanin, diosgenin, rutin, sarsasapogenin, and shatavarin A was

calculated as 5.969, 6.124, 2.983, 6.671, and 6.676 eV, respectively. The band gap of rutin was minimal among the other selected phytochemicals. The low band gap supports the higher and easy excitation of the electrons during the charge excitation which shows the good sustainability with the chemical reactivity. The rest of the phytochemicals have large amounts of band gap which shows their low chemical reactivity. On the contrary, these phytochemicals favor conductivity to a lesser extent and are considered to be insulators. In a similar context, both the IP (ability of the nucleophile to donate the charge cloud) and EA (energy required by electrophile to withdraw the donated charge) values of rutin were greater than the rest of the selected phytochemicals. This supports the high chemical reactivity of rutin. The negative value of CP shows the potential to carry out chemical reactions. More negativity leads to enhanced ability of the molecule to participate in the chemical reactions. A similar kind of interpretation can be made using the chemical hardness (η). The less the η is, the more will be the flexibility of the compound for the chemical reactions. In pharmaceutics, a drug must have the potential to be taken as a combination of different other drugs for which a compound must have high chemical reactivity. From the FMO analysis, it was clear that rutin was highly reactive among the other selected phytochemicals. The MEP surfaces were also plotted and illustrated in Figure 3. The red regions showed the electrophilic part and the blue color indicates the nucleophilic part in the molecules (Mali et al., 2022). The more the intensity of the color, the more will be the nature of nucleophilic and electrophilic moieties. In asparanin, the O-H bonds act as both nucleophilic and electrophilic depending upon the variation in the charge. In diosgenin and rutin, the strong electrophilic and nucleophilic nature is visible due to the intense color of the blue and red color surfaces. In shatavarin A, there seems a low electrophilic nature as the light-yellow color was visible. Ultimately, the MEP surface indicates the strong intramolecular charge transfer in diosgenin and rutin. Similar dislocation of the charge cloud from HOMO to LUMO was noticed from the molecular orbital surfaces analysis (Figure 4). Thus, the DFT was well suited to express the chemical reactivity of the selected phytochemicals and rutin was the most reactive molecule among the selected phytochemicals.

Table 2. Global reactivity parameters for the phytochemicals

Property	Asparanin	Diosgenin	Rutin	Sarsasapogenin	Shatavarin A
HOMO	-7.020	-6.501	-8.056	-7.047	-8.923
LUMO	-1.051	-0.377	-5.073	-0.376	-2.156
ΔE	5.969	6.124	2.983	6.671	6.767
IP	7.020	6.501	8.056	7.047	8.923
EA	1.051	0.377	5.073	0.376	2.156
CP	-4.035	-3.439	-6.564	-3.715	-5.539
χ	4.035	3.439	6.564	3.715	5.539
η	2.985	3.062	1.491	3.335	3.383

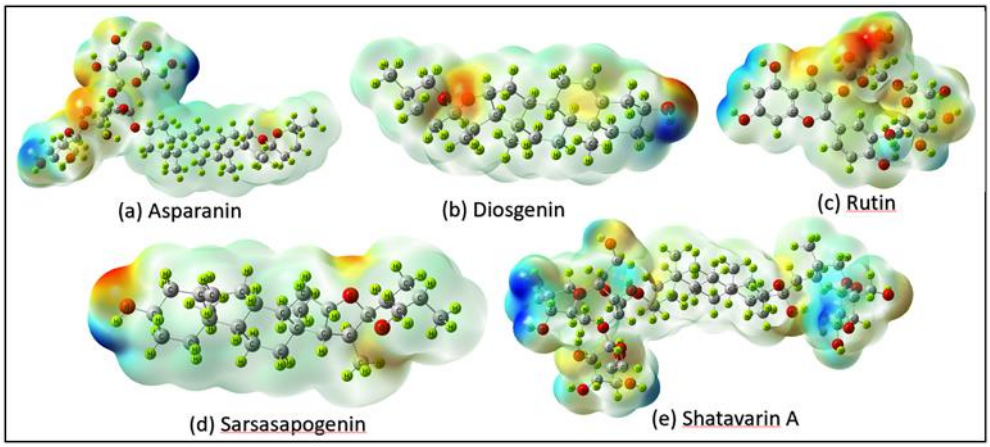

Figure 3. Molecular electrostatic potential (MEP) surfaces indicate the chemically reactive sites in the phytochemicals

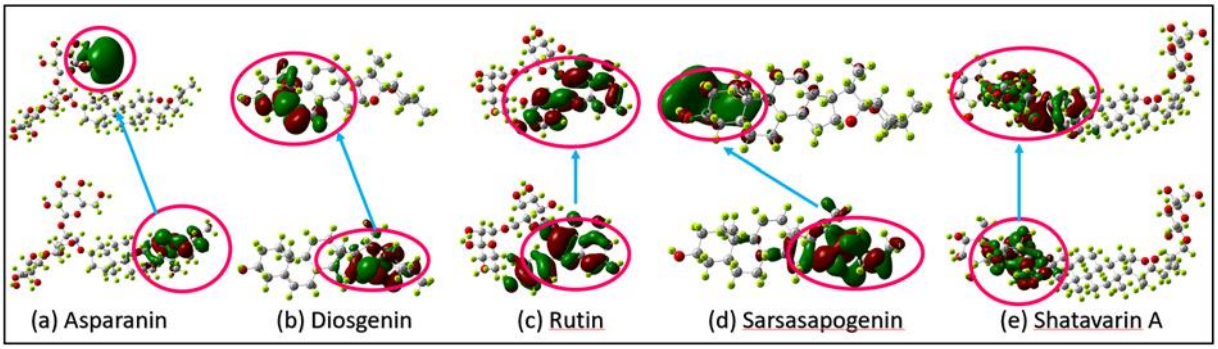

Figure 4. HOMO-LUMO surfaces indicate the occurrence of charge transfer by dislocation of the orbital surfaces

3.3. Physiochemical properties

The physiochemical properties of the selected phytochemicals were analyzed and are mentioned in supplementary file SD 4. As per Lipinski's rule, the molecular weight of the drug-like molecule must be less than 500 g/mol. According to this, diosgenin, and sarsasapogenin have the molecular weight of 414.63 and 416.65 g/mol. LogP is a property of how hydrophilic or hydrophobic a drug-like molecule is. The higher the value of LogP, the higher will be the hydrophilic nature of the molecule and the higher will be the absorbent rate of the drug in the human body. diosgenin, and sarsasapogenin, both have high values of LogP of 5.71 and 5.79 respectively. The TPSA is the quantitative measure of the biological area that comprises oxygen, nitrogen, and hydrogen atoms (Rashid et al., 2022). The value of the TPSA must be low to give better binding affinity. The polar hydrogen atoms are often retained during the preparation step of the proteins as the availability of polar hydrogens is important in terms of intermolecular interactions. Nevertheless, among the selected best phytochemicals, diosgenin, and sarsasapogenin have a minimum and equal topological polar surface area of 38.69 Å2. Similar to this context, the hydrogen bond donors and acceptors, carbon atoms, and heavy atoms were low for diosgenin and sarsasapogenin. Only three heteroatoms were present in diosgenin and sarsasapogenin and higher for the rest of the three phytochemicals. Rotatable bonds are absent in diosgenin and sarsasapogenin. Lipinski's rule of 5 restricts the drug-like molecules to have several rotatable bonds of less than 10. Therefore, all the mentioned physiochemical properties established the potential drug-like nature of diosgenin and sarsasapogenin among the five phytochemicals.

3.4. Drug-likeness and ADMET analysis

The drug-like properties like Lipinski's rule of 5, Ghose, Veber, Egan, Mugge, etc. rules were considered for the asparanin, diosgenin, rutin, sarsasapogenin, and shatavarin A (Table 3). Among these phytochemicals, diosgenin, and sarsasapogenin have a minimum number (1) of violations of Lipinski's rule of 5 which makes them potential candidates that follow this rule. Apart from diosgenin and sarsasapogenin, the other three phytochemicals asparanin, rutin, and shatavarin A have three Lipinski violations each. Veber's rule and Egan's rule were also followed by diosgenin and sarsasapogenin. The high value of the quantitative estimate of drug-likeness (QEDw) score makes it a potential drug-like. Similar phytochemicals with minimum drug-like rules violation have a high score weighted QEDw score. Diosgenin and sarsasapogenin showed high values of QED scores of 0.52 and 0.54, respectively. Thus, the drug-like analysis reveals that among the chosen phytochemicals with high binding affinity, diosgenin and sarsasapogenin follow the drug-like properties most favorably and are potential drug-like molecules.

Table 3. Drug-like and ADMET properties of the phytochemicals

Property name	Asparanin	Diosgenin	Rutin	Sarsasapogenin	Shatavarin A
Number of Lipinski's rule of 5 violations	3	1	3	1	3
Lipinski's rule of 5	Failed	Passed	Failed	Passed	Failed
Veber rule	Bad	Good	Bad	Good	Bad
Egan rule	Bad	Good	Bad	Good	Bad
Weighted quantitative estimate of drug-likeness (QEDw) score	0.15	0.52	0.14	0.54	0.07
Bioavailability score	0.17	0.55	0.17	0.55	0.17
Solubility class [ESOL]	Moderately soluble	Moderately soluble	Soluble	Poorly soluble	Moderately soluble
Solubility class [Silicos-IT]	Soluble	Moderately soluble	Soluble	Moderately soluble	Soluble
Blood-brain barrier permeation	No	Yes	No	Yes	No
Gastrointestinal absorption	Low	High	Low	High	Low
Log K_p (Skin permeation, cm/s)	-10.53	-4.8	-10.26	-4.23	-12.88

The ADMET properties of the phytochemicals were analyzed for all the selected phytochemicals. A high bioavailability score of diosgenin and sarsasapogenin was noticed. Both these phytochemicals were found to obey most of the ADMET properties. High blood-brain-barrier penetration was observed in diosgenin and sarsasapogenin. This means these phytochemicals have better capability to get into the blood-brain stream and could have better absorption in the body of the patient. Similarly, the gastrointestinal absorption of these phytochemicals diosgenin and sarsasapogenin was observed to be high which results in the high absorption of the drugs in the patient's intestines. The better the absorption of the drug in the human body, the better will it target the relevant tissue and the better the drug will show its pharmacodynamic activity. The higher value of Log Kp i.e., skin permeation, increases the value of blood vessels in the skin and enriches the availability of oxygen and nutrients in the tissue. This phenomenon is called vascularization. The higher the possibility of vascularization, the higher the druggability of the compound. Therefore, diosgenin and sarsasapogenin have better skin permeation in the human body. Hence, from drug-like and ADMET analysis, diosgenin and sarsasapogenin show the best drug-like behavior and have better druggability as inhibitors against any disease.

3.5. Cardiotoxicity analysis

The cardiotoxicity map of the phytochemicals was studied to check the nature and responses of the phytochemicals towards cardio-health. The cardio-toxicity map of all the considered phytochemicals was mentioned in supplementary file SD 5. The positive value of potential cardiotoxicity indicates the favored behavior of the molecule to the cardiotoxicity. Additionally, the negative value shows the shielding from the cardiotoxicity. The pink-colored areas in the probability map are the regions that inhibit the effect on the human heart. Among all the considered phytochemicals, D-galacturonic acid, and D-glucose were within the most highlighted pink-colored areas that show these two phytochemicals as strong candidates as non-cardiotoxic. D-galacturonic acid, D-glucose, hyperoside, kaempferol, quercetin, and quercetin 3-*O*-glucuronide were phytochemicals which are strong non-cardiotoxic substances and have a value of applicability domain of 0.14, 0.11, 0.2, 0.19, 0.19, and 0.2, respectively. Apart from these phytochemicals, the applicability domain values of asparanin, cyanin, diosgenin, rutin, sarsasapogenin, and stigmasterol were 0.17, 0.19, 0.18, 0.2, 0.16, and 0.2, respectively. These phytochemicals showed an applicability domain near to that of non-cardiotoxic features and thus are not at such extreme case of cardiotoxicity in the human body after consumption.

3.6. Post docking analysis

The post-docking analysis was done to further study the nature of the docking between the inhibitor and the receptor. This was studied for only diosgenin and sarsasapogenin, the two phytocompounds for which all the physiochemical, drug-like, and ADMET properties were the most favorable. The interactions of the docking between diosgenin and sarsasapogenin and all the proteins have been shown in Figure 5. The docking details of all the protein-ligand complexes of diosgenin, and sarsasapogenin, have been listed in supplementary file SD 6 and 7. Mainly the carbon-hydrogen bond, conventional hydrogen bond interactions, pi-alkyl bond, and pi-sigma bond were seen to be involved in the protein-ligand interactions. The amino acid interactions of diosgenin and sarsasapogenin are illustrated in Figure 6 and 7. The association of amino acid residues such as proline (PRO), alanine (ALA), tryptophan (TRP), arginine (ARG), cysteine (CYS), lysine (LYS), glutamine (GLN), valine (VAL), histidine (HIS), glycine (GLY), leucine (LEU), asparagine (ASN), serine (SER), tyrosine (TYR), aspartic acid (ASP), and isoleucine (ILE) was found at the protein-ligand interaction interface of diosgenin and sarsasapogenin.

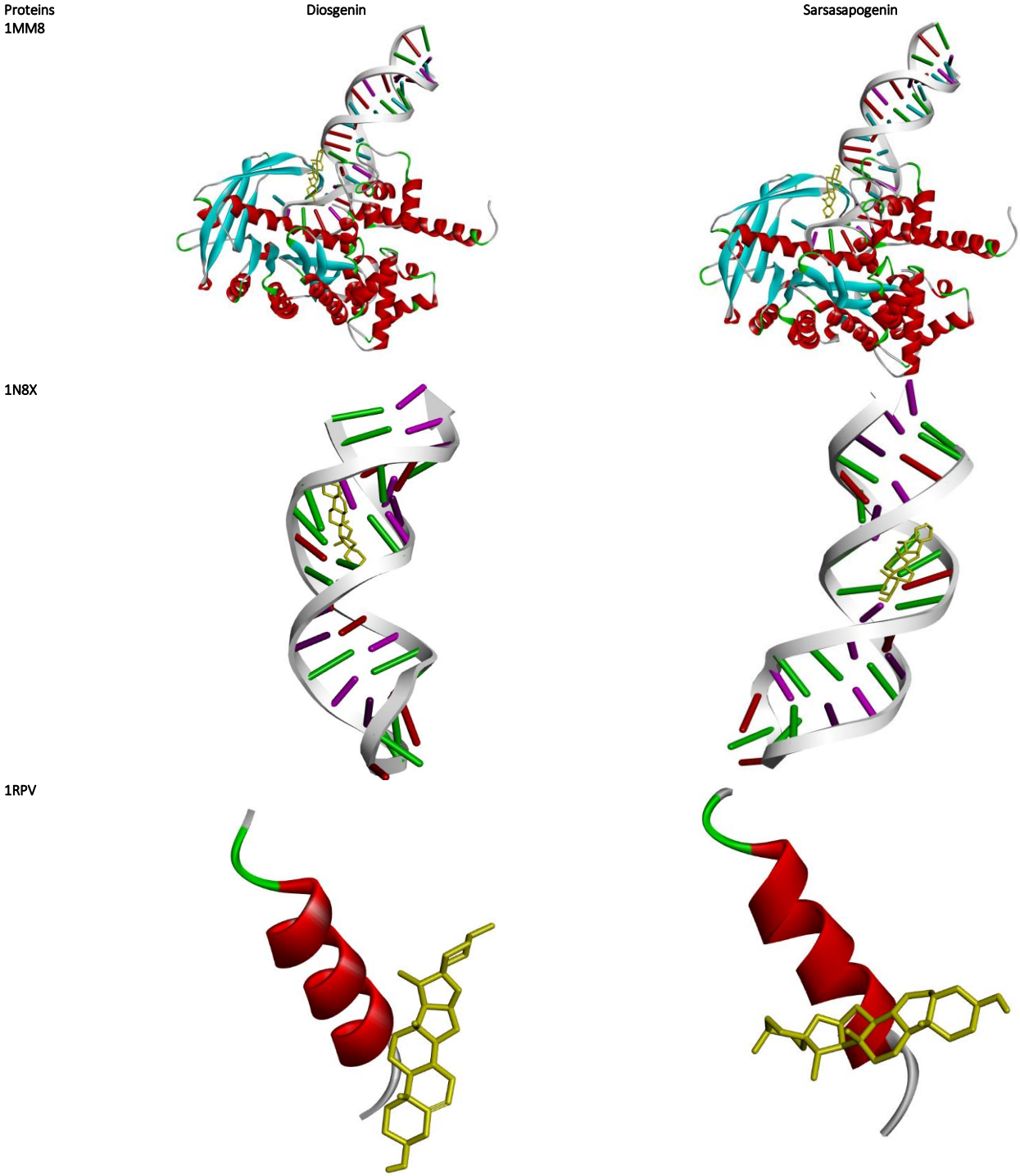

1RZJ

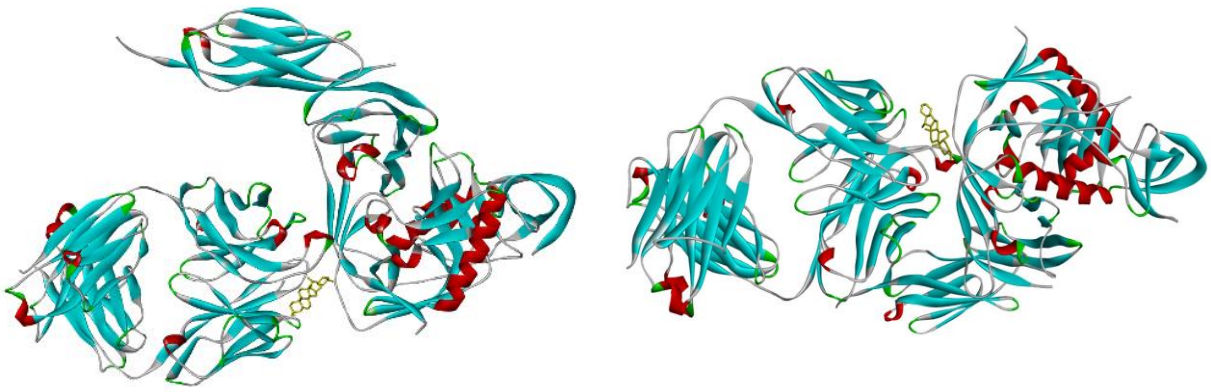

1TVR

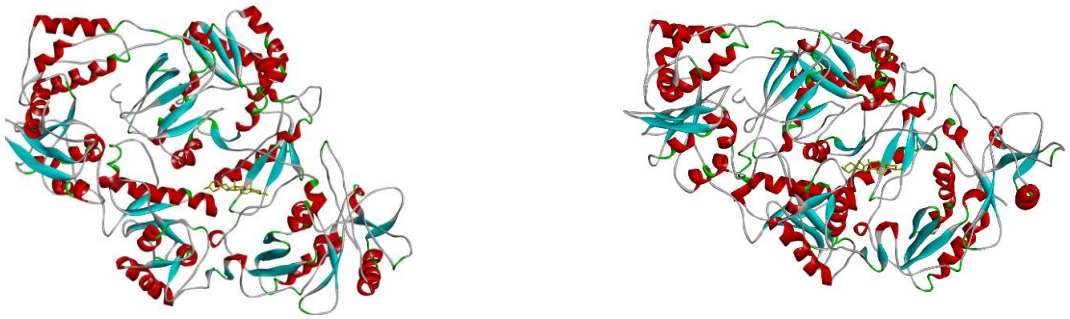

1UWB

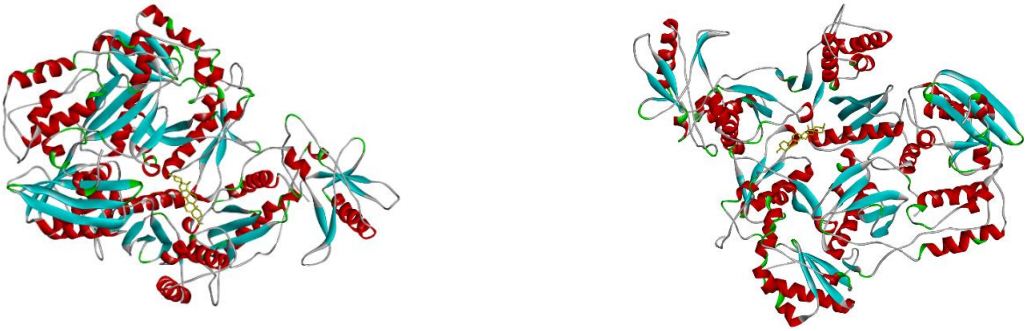

3DIK

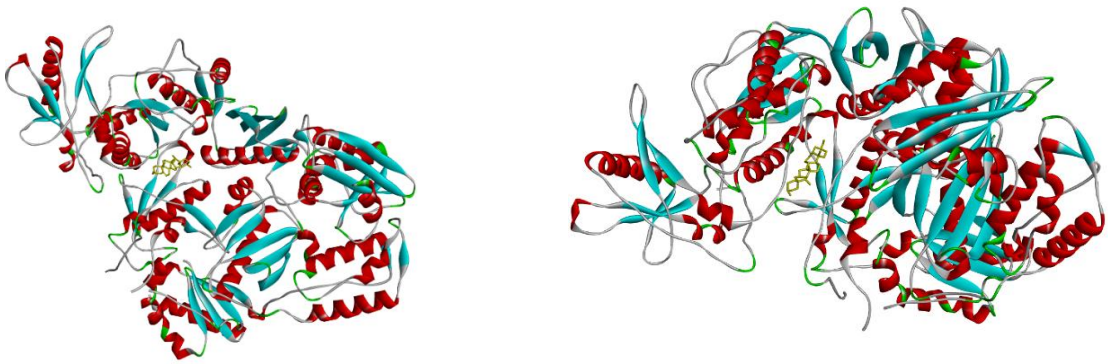

4P6A

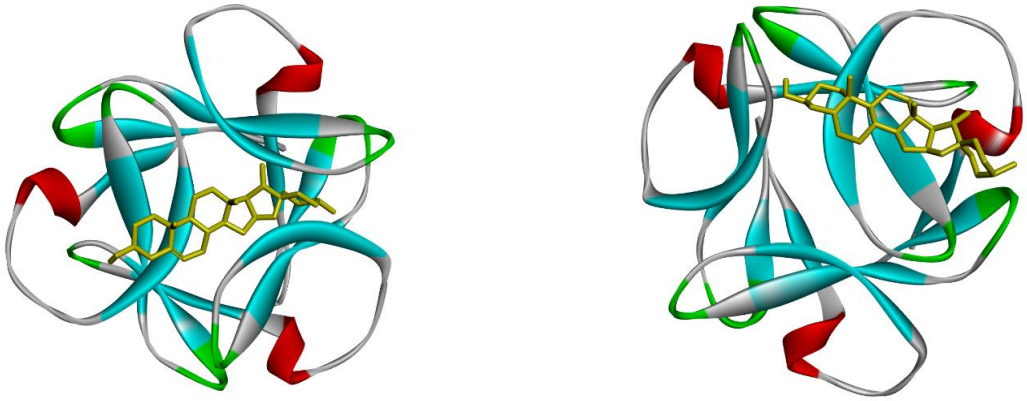

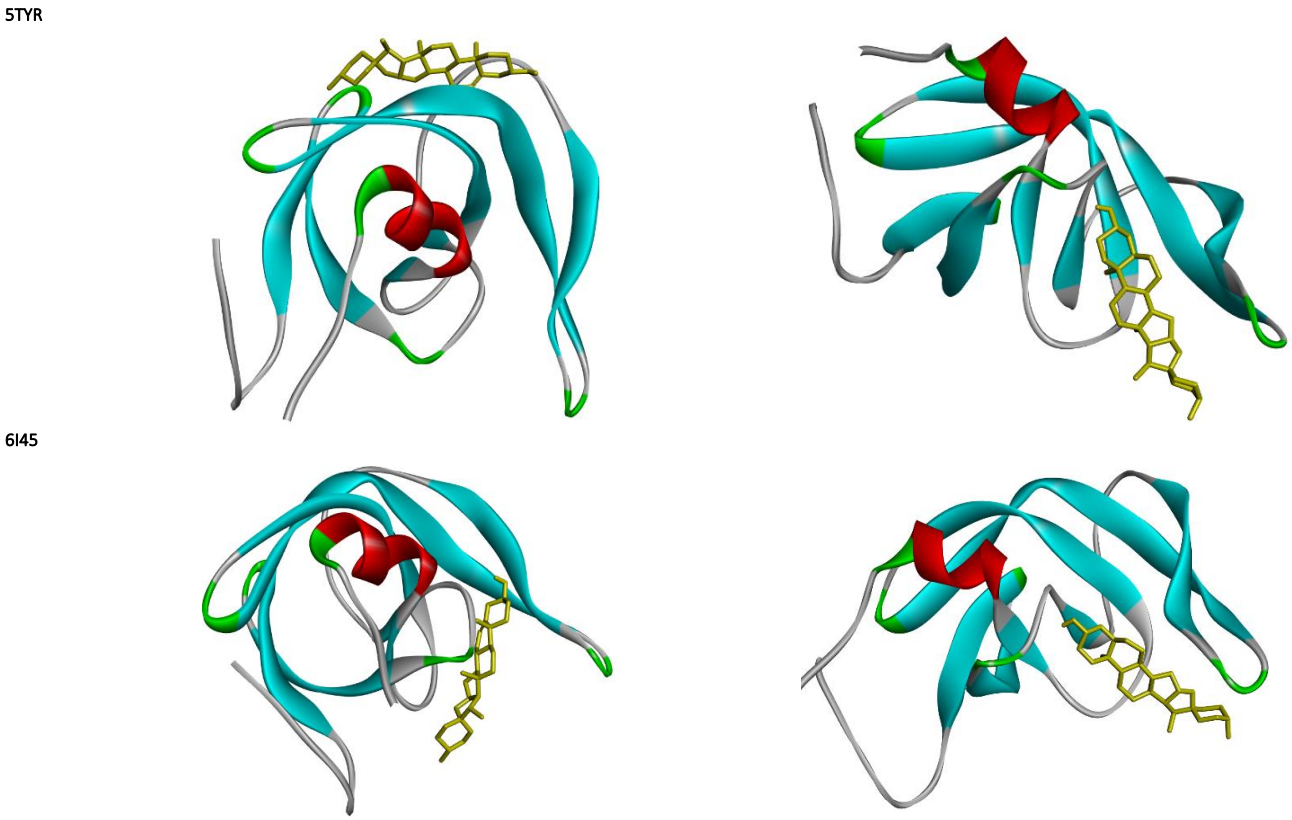

Figure 5. Location of the diosgenin and sarsasapogenin at the binding sites of the target macromolecules

For 1MM8, diosgenin formed two hydrogen bonds (DCC:205 and DAB:113) and three hydrophobic contacts (LYS A:439 and PRO A:242) noticed on the binding site with an inhibition constant of 2.44×10^{-7}. The hydrogen bond and hydrophobic interactions for sarsasapogenin docked with 1MM8 were three (PRO A:242, LYS A:439, and ALA A:258) and two (DC C:205 and DA B:113), respectively, with an inhibition constant of 4.05×10^{-7}. Sarsasapogenin showed better intermolecular interactions with the binding site of 1MM8.

While, for 1N8X, diosgenin has a binding affinity of -9.7 kcal/mol with an inhibition constant of 1.74×10^{-7} and a dipole moment of 2.343 Debye. Furthermore, diosgenin showed two hydrogen bonds (GA:26 and AA:27) and one hydrophobic contact (GA:28), respectively. For the same protein, sarsasapogenin has a binding affinity of -9.5 kcal/mol, formed two hydrogen bonds (GA:28 and AA:25), and one pi-alkyl hydrophobic interaction (GA:26). Sarsasapogenin showed an inhibition constant of 1.05×10^{-7}, and a dipole moment of 2.309 Debye. Thus, for 1N8X, diosgenin was found to have better binding interactions as compared to sarsasapogenin.

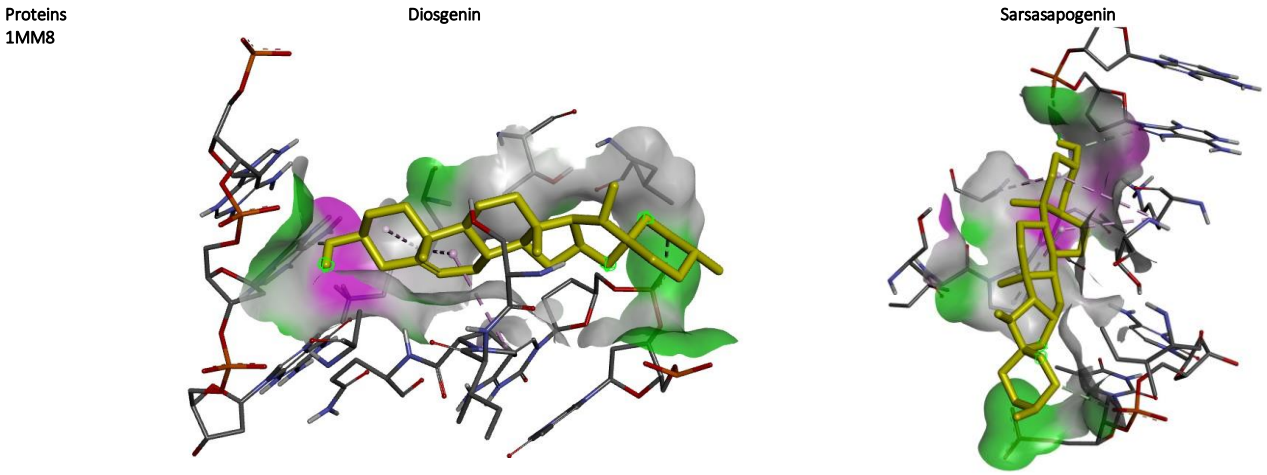

1N8X

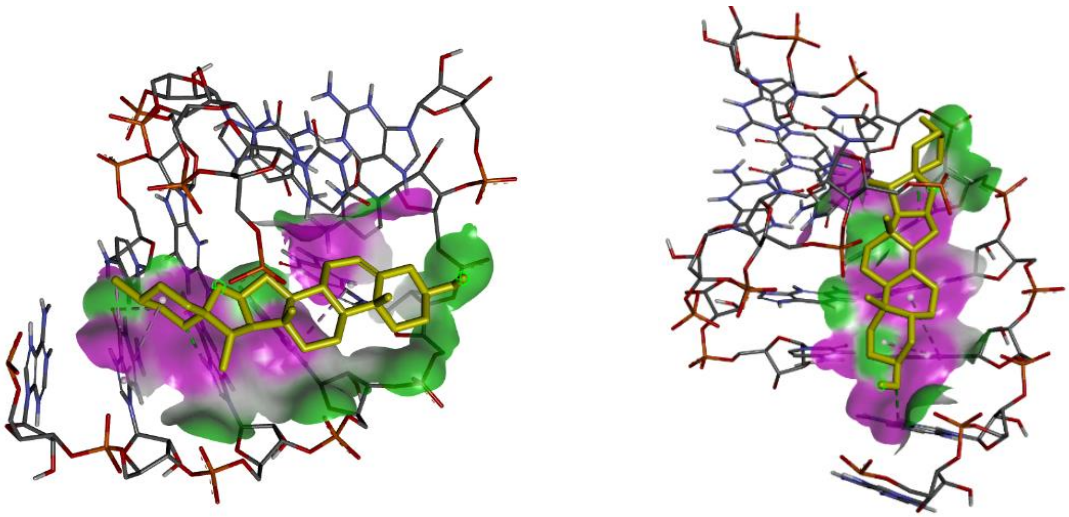

1RPV

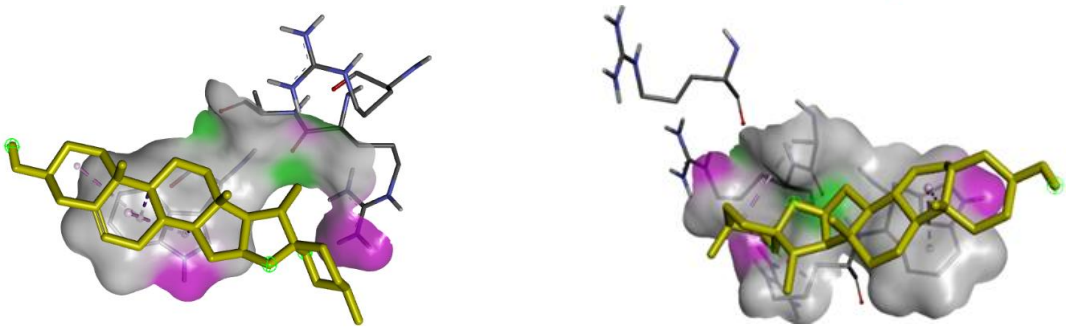

1RZJ

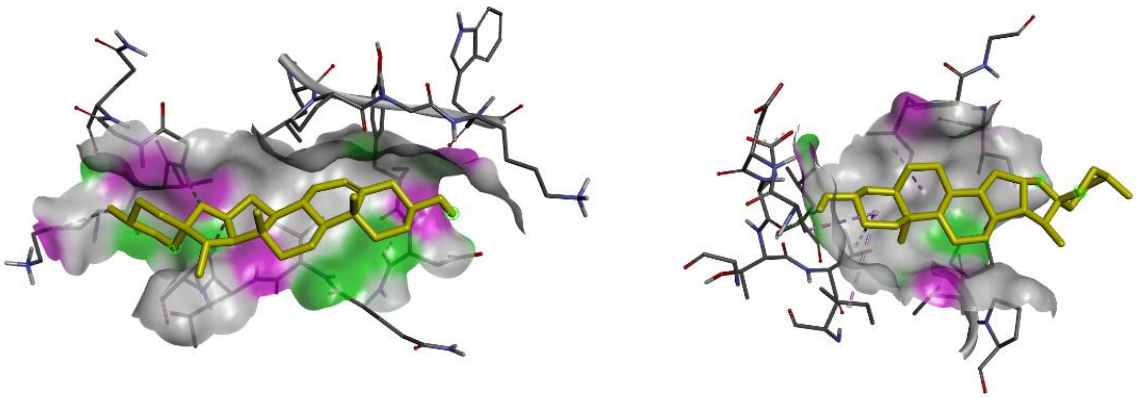

1TVR

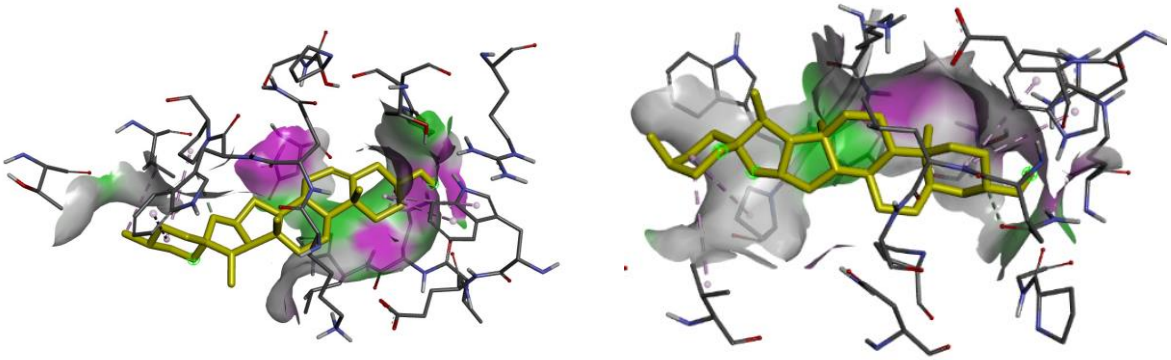

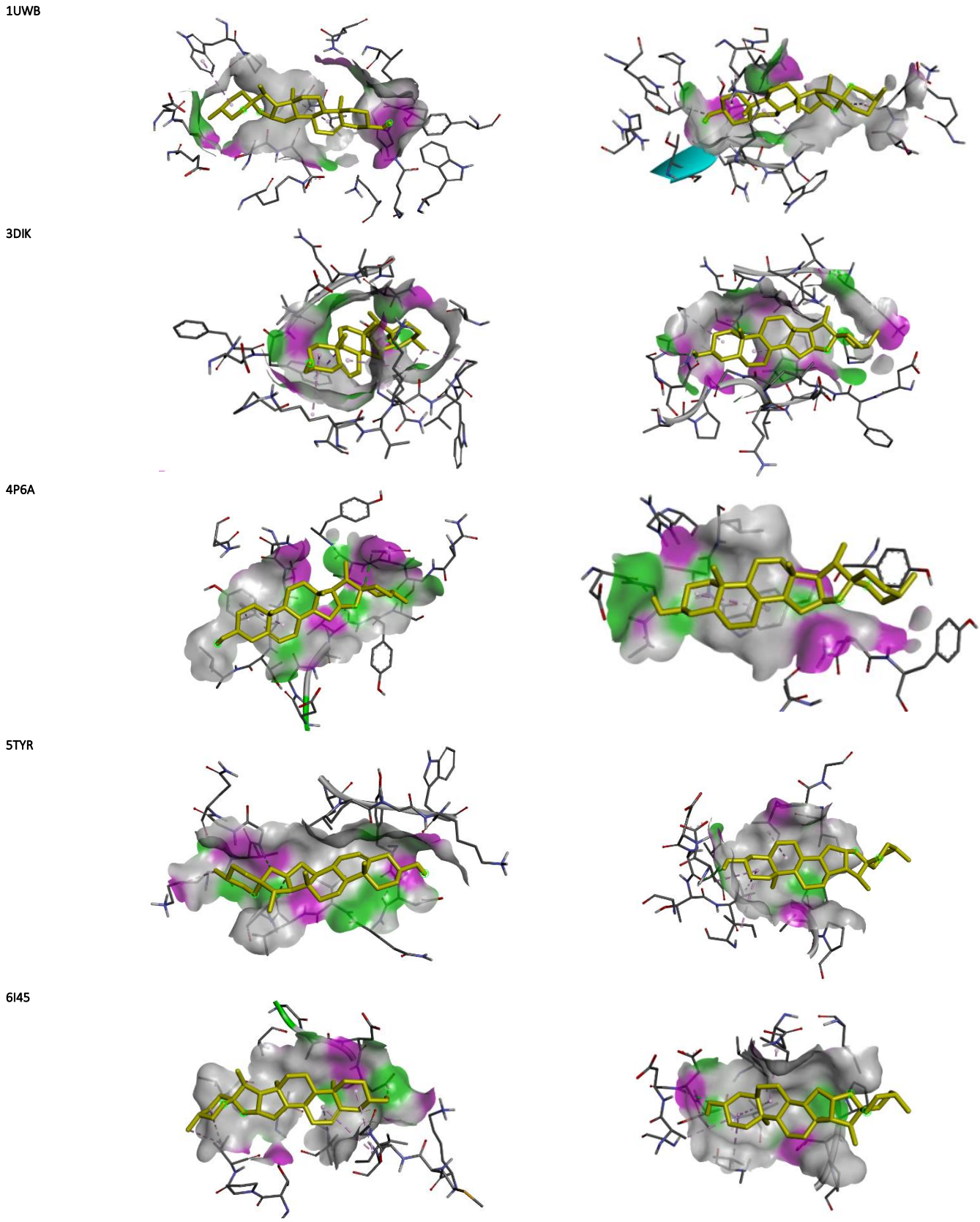

Figure 6. 3-D visualization of the binding profile of the inhibitor-receptor complex with the indication of the donor-acceptor regions of the binding site (pink-donor and green-acceptor)

The alternative binding conformation of diosgenin with 1RPV was characterized by a binding affinity of -6.3 kcal/mol, a dipole moment of 2.2 Debye, the formation of four hydrophobic contacts with the TRP A:13 residue, with an inhibition constant of 2.34×10^{-5}. Likewise, the best docking pose for sarsasapogenin against 1RPV was identified as the second binding configuration, characterized by a binding affinity of -6.2 kcal/mol, a dipole moment of 2.069 Debye, an inhibition constant of 2.78×10^{-5}, the formation of one hydrogen

bond with ALA A:10, and four hydrophobic contacts, including two with ARG A:14 and two with TRP A:13. The more favorable binding affinity and dipole moment established diosgenin as the most effective inhibitor of 1RPV.

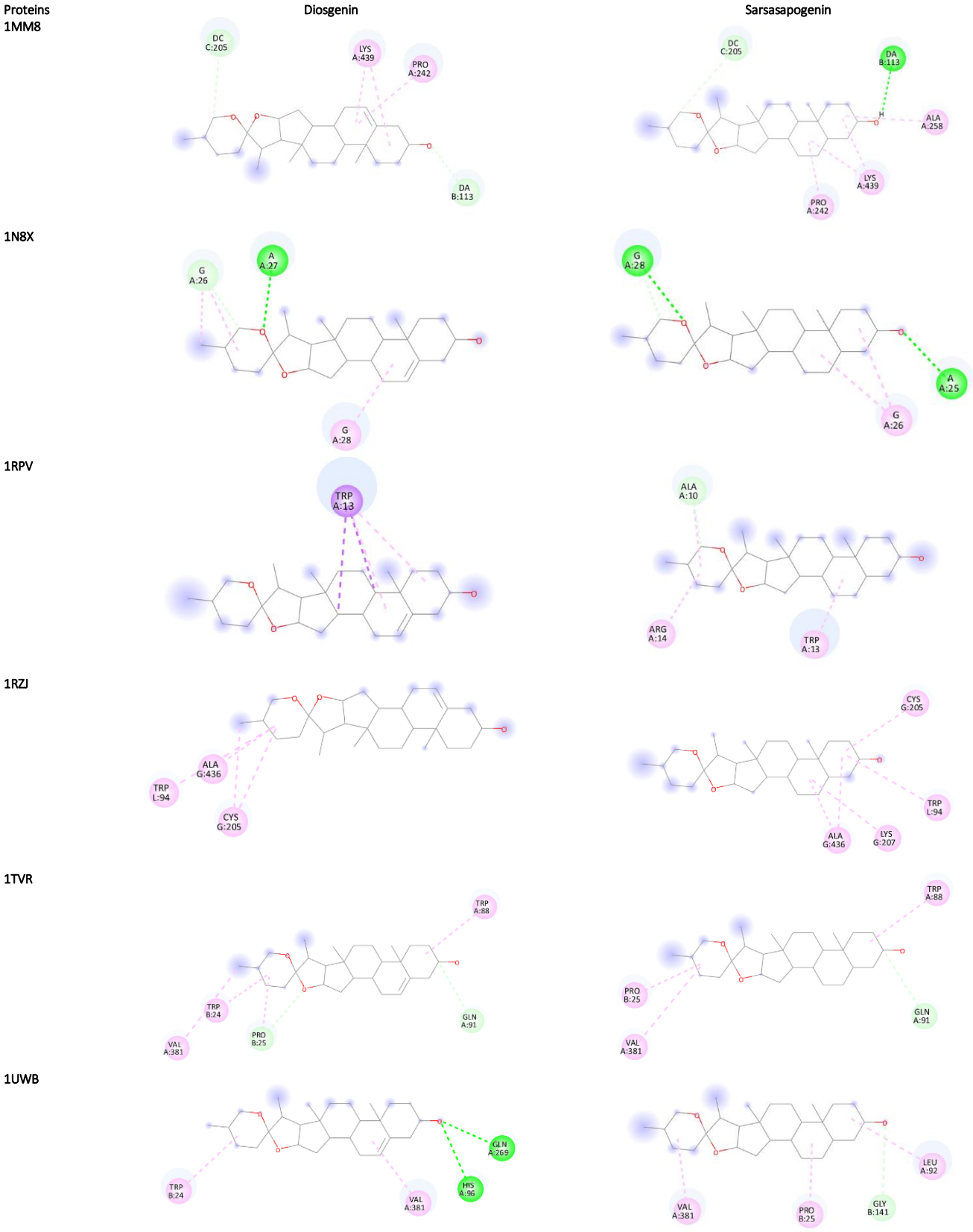

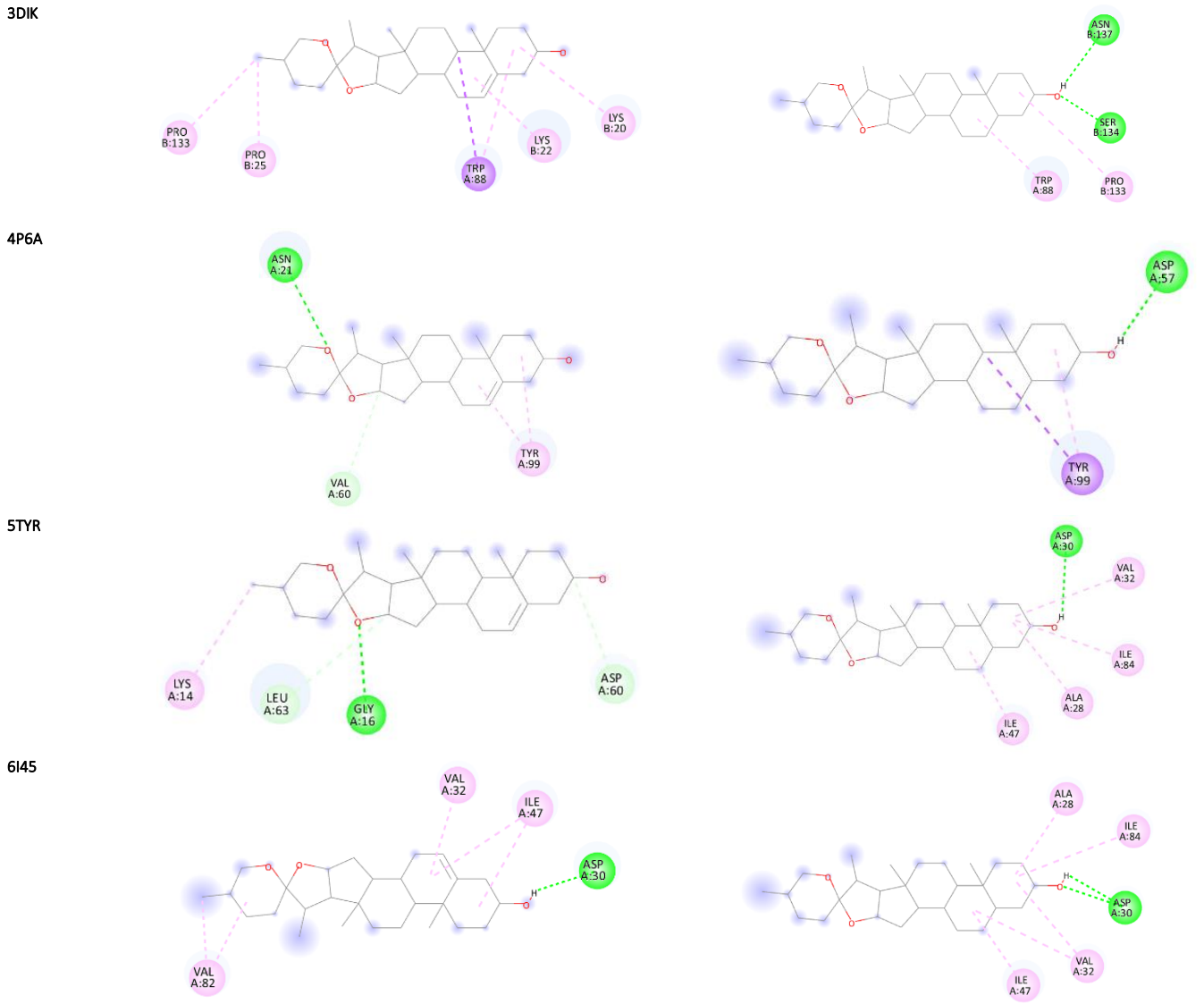

Figure 7. 2-D illustration of the amino acid interactions of the binding profile of the inhibitor-receptor complex
Light green: carbon-hydrogen bond, Dark green: conventional hydrogen bond interactions, Pink: pi-alkyl bond, Purple: pi-sigma bond

Diosgenin gave the best binding affinity of -10.5 kcal/mol for 1RZJ with four hydrophobic contacts including two with ALA G:436 and one each with TRP L:94 and CYS G:205 involved in the binding and diosgenin showed a calculated inhibition constant of 4.45×10^{-6}. For this protein, the fifth pose of sarsasapogenin with a binding affinity of -8.4 kcal/mol has an inhibition constant of 6.72×10^{-7} with five hydrophobic contacts (CYS G:205, TRP L:94, LYS G:207, and ALA G:436). Based on a high count of hydrophobic interactions, and higher inhibition constant, sarsasapogenin was a better binder at the binding site with the 1RZJ.

The third mode of diosgenin with 1TVR showed a binding affinity of -9.3 kcal/mol, an inhibition constant of 1.47×10^{-7}, two hydrogen bond (PRO B:25 and GLN A:269) interactions, and five hydrophobic contacts (VAL A:381, TRP B:24, and TRP A:88). The second binding mode of sarsasapogenin with 1TVR showed the same binding affinity of -9.3 kcal/mol, an inhibition constant of 1.47×10^{-7}, one hydrogen bond (GLN A:91), and four hydrophobic contacts (TRP A:88, PRO B:25, and VAL A:381). The dipole moment, binding affinity, and inhibition constant of both the phytochemicals with 1TVR were more or less within the same range for the hydrogen bond and hydrophobic interactions. Thus, the higher number of hydrogen bond interactions highlight diosgenin a better inhibitor of 1TVR compared to sarsasapogenin.

For 1UWB, the fourth pose showed a binding affinity of -8.2 kcal/mol, one hydrogen bond (HIS A:96 and GLN A:269) interaction, and two hydrophobic contacts (TRP B:24 and VAL A:381). The inhibition constant of this binding mode was 9.43×10^{-7}. Sarsasapogenin showed a more favorable binding affinity of -8.7 kcal/mol for 1UWB with one hydrogen bond (GLY B:141), three hydrophobic contacts (VAL A:381, PRO B:25, and LEU A:92), and an inhibition constant of 4.05×10^{-7}. Sarsasapogenin, therefore, was more promising based on inhibitory interactions with 1UWB compared to that of diosgenin.

Subsequent to its binding to 1RZJ, diosgenin demonstrates a notable binding strength of -10.4 kcal/mol against 3DIK, characterized by the formation of six hydrophobic contacts. In contrast, sarsasapogenin exhibits a binding affinity of -9.4 kcal/mol with 3DIK, involving two hydrogen bonds (ASN B:137 and SER B:134) as well as hydrophobic contacts with TRP A:88 and PRO B:133, respectively. The stronger binding affinity and the increased number of hydrophobic contacts

associated with diosgenin suggest this ligand as a superior inhibitor of 1RZJ compared to sarsasapogenin.

The top-ranked binding conformation of diosgenin, yielding a binding affinity of -8.3 kcal/mol when docked with 4P6A, involves interactions via two hydrogen bonds (VAL A:60 and ASN A:21) and hydrophobic contacts with TYR A:99. The resultant inhibition constant was found to be 7.96×10^{-7}, accompanied by a dipole moment of 1.17 Debye. In the case of sarsasapogenin, the third-ranked docking pose with 4P6A, characterized by a binding affinity of -7.7 kcal/mol, shows a dipole moment of 2.28 Debye, an inhibition constant of 2.2×10^{-7}, a single hydrogen bond (ASP A:57), and two hydrophobic contacts with TYR A:99. This comparative analysis underscores the promising binding of diosgenin with 4P6A.

Regarding the interaction with 5TYR, diosgenin shows a good binding affinity of -8.8 kcal/mol, characterized by the formation of three hydrogen bonds (LEU A:63, GLY A:16, and ASP A:60) and one hydrophobic contact with LYS A:14. The inhibition constant for diosgenin was calculated as 3.42×10^{-7}. In comparison, sarsasapogenin exhibits a binding affinity of -7.6 kcal/mol with 5TYR, forming one hydrogen bond with ASP A:30, along with four hydrophobic contacts involving VAL A:32, ILE A:84, ALA A:28, and ILE A:47. The inhibition constant for sarsasapogenin was calculated as 2.6×10^{-6}. These molecular attributes of diosgenin, regarding its high binding affinity, hydrogen bonding interactions, and lower inhibition constant, underscore its optimal binding with 5TYR.

The sixth best-ranked binding mode of diosgenin showed the best binding with 6I45 (-7.4 kcal/mol) with a dipole moment of 2.293 Debye, an inhibition constant 3.65×10^{-6}, and five hydrophobic contacts (two with ILE A:47, two with VAL A:82 each and one with VAL A:32) and one hydrogen bond with ASP A:30. For sarsasapogenin, the binding affinity was -7.6 kcal/mol, a dipole moment of 2.219 Debye, an inhibition constant of 2.6×10^{-6}, two hydrogen bonds with ASP A:30, and five hydrophobic contacts with ALA A:28, ILE A:84, ILE A:47, and two with ASP A:30. The better dipole moment and inhibition constant of diosgenin revealed its better binding with 6I45.

Hence, the post-docking analysis reveals promising inhibitory interactions between diosgenin and sarsasapogenin against several HIV proteins. Specifically, diosgenin exhibits inhibitory potential against 1N8X, 1RPV, 1TVR, 3DIK, 4P6A, 5TYR, and 6I45, while sarsasapogenin demonstrates inhibitory interactions against 1MM8, 1RZJ, and 1UWB proteins among the evaluated target receptors.

4. Conclusions

The present study reports the detailed quantum chemical study of the phytoconstituents of *A. racemosus*. The molecular docking performed for all the phytochemicals reveals the best binding scores for asparanin, diosgenin, rutin, sarsasapogenin, and shatavarin A. The drug-like and ADMET analysis was done for these five phytochemicals and the ADMET analysis suggested that the diosgenin and sarsasapogenin were the best phytochemicals with most of the ADMET and physiochemical properties followed. The ADMET analysis reveals that these two phytochemicals are ideal drug-like molecules and could further be employed as anti-HIV drugs. The reactivity analysis performed for the selected phytochemicals reveals the high chemical reactivity of the selected phytochemicals. The post-docking analysis carried out for diosgenin and sarsasapogenin reveals that these two phytochemicals are the best for preventing the replication of the prominent HIV-AIDS target macromolecules. The protein-ligand interactions in the case of diosgenin and sarsasapogenin have an association of carbon-hydrogen bonds, conventional hydrogen bond interactions, pi-alkyl and pi-sigma contacts. The formation of these kind of interactions supports the strong interaction between the inhibitor and the receptors in case of diosgenin and sarsasapogenin. The computational predictions performed for the inhibitory activity of diosgenin and sarsasapogenin provide a reliable basis for potential exploration in clinical drug development using these compounds. There could be interpreted as the leaf (enriched with diosgenin) and fruit (enriched with sarsasapogenin) may have the potential to act as herbal aids against HIV, though further experimental research is warranted to confirm and elaborate on these findings.

Acknowledgments

None.

Conflict of interest

The authors declare that they have no known competing financial interests or personal relationships that could have appeared to influence the work reported in this paper.

Statement of ethics

In this study, no method requiring the permission of the "Ethics Committee" was used.

Availability of data and materials

All data generated or analyzed during this study, which support the plots within this paper and the other findings of this study, are included in this article and its supplementary file. Source data are provided in this paper.

Funding

M. Rana thanks Uttarakhand State Council for Science & Technology (UCOST), Department of Information and Science Technology, Government of Uttarakhand, for financial support through an R&D Research Project (Project no: UCS&T/R&D-42/22-23/23603/1).

CRediT authorship contribution statement

Meenakshi Rana: Conceptualization, Methodology, Writing-Reviewing and editing, Supervision
Shradha Lakhera: Data curation, Writing-original draft preparation, Visualization, Investigation, Software, Validation
Kamal Devlal: Conceptualization, Writing- reviewing and editing

ORCID Numbers of the Authors

M. Rana: 0000-0002-9156-9125
S. Lakhera: 0009-0004-5962-4667
K. Devlal: 0000-0002-5639-3822

Supplementary File

The supplementary file accompanying this article is available at https://life-insilico.com/index.php/pub/libraryFiles/downloadPublic/9.

Publisher's Note

All claims expressed in this article are solely those of the authors and do not necessarily represent those of their affiliated organizations, or those of the publisher, the editors and the reviewers. Any product that may be evaluated in this article, or claim that may be made by its manufacturer, is not guaranteed or endorsed by the publisher.

References

Agrawal, M., Tripathi, D. K., Saraf, S., Saraf, S., Antimisiaris, S. G., Mourtas, S., Hammarlund-Udenaes, M., & Alexander, A. (2017). Recent advancements in liposomes targeting strategies to cross blood-brain barrier (BBB) for the treatment of Alzheimer's disease. *Journal of Controlled Release, 260*, 61-77.

Alok, S., Jain, S. K., Verma, A., Kumar, M., Mahor, A., & Sabharwal, M. (2013). Plant profile, phytochemistry and pharmacology of *Asparagus racemosus* (Shatavari): A review. *Asian Pacific Journal of Tropical Disease, 3*(3), 242-251.

Baev, A. K. (2012). Reverse Dative Bond in Organic Compounds, Molecular Complexes and Inconsistency of the sp 3-Hybridization Model with Respect to Carbon Atom. In A. K. Baev (Ed.), *Specific Intermolecular Interactions of Organic Compounds* (pp. 1-28): Springer, Berlin, Heidelberg.

Baker, D. D., Chu, M., Oza, U., & Rajgarhia, V. (2007). The value of natural products to future pharmaceutical discovery. *Natural Product Reports, 24*(6), 1225-1244.

Bharadvaja, N. (2023). Exploring different computational approaches for effective diagnosis of breast cancer. *Progress in Biophysics and Molecular Biology, 177*, 141-150.

Chen, Y., Ye, D., Held, M. A., Cannon, M. C., Ray, T., Saha, P., Frye, A. N., Mort, A. J., & Kieliszewski, M. J. (2015). Identification of the abundant hydroxyproline-rich glycoproteins in the root walls of wild-type *Arabidopsis*, an ext3 mutant line, and its phenotypic revertant. *Plants, 4*(1), 85-111.

Chikhale, R. V., Sinha, S. K., Patil, R. B., Prasad, S. K., Shakya, A., Gurav, N., Prasad, R., Dhaswadikar, S. R., Wanjari, M., *et al.* (2021). In-silico investigation of phytochemicals from *Asparagus racemosus* as plausible antiviral agent in COVID-19. *Journal of Biomolecular Structure and Dynamics, 39*(14), 5033-5047.

Delelis, O., Carayon, K., Saïb, A., Deprez, E., & Mouscadet, J. F. (2008). Integrase and integration: biochemical activities of HIV-1 integrase. *Retrovirology, 5*(1), 1-13.

Du, S., Betts, L., Yang, R., Shi, H., Concel, J., Ahn, J., Aiken, C., Zhang, P., & Yeh, J. I. (2011). Structure of the HIV-1 full-length capsid protein in a conformationally trapped unassembled state induced by small-molecule binding. *Journal of Molecular Biology, 406*(3), 371-386.

Gillespie, S. L., Chinen, J., Paul, M. E., & Shearer, W. T. (2019). Human immunodeficiency virus infection and acquired immunodeficiency syndrome. In R. R. Robert, T. A. Fleisher, W. T. Shearer, H. W. Schroeder, A. J. Frew, & C. M. Weyand (Eds.), *Clinical Immunology (Fifth Edition)* (pp. 545-560): Elsevier Ltd.

Gorgulla, C., Boeszoermenyi, A., Wang, Z. F., Fischer, P. D., Coote, P. W., Padmanabha Das, K. M., Malets, Y. S., Radchenko, D. S., Moroz, Y. S., *et al.* (2020). An open-source drug discovery platform enables ultra-large virtual screens. *Nature, 580*(7805), 663-668.

Hosen, M. A., El Bakri, Y., Rehman, H. M., Hashem, H. E., Saki, M., & Kawsar, S. M. (2023). A computational investigation of galactopyranoside esters as antimicrobial agents through antiviral, molecular docking, molecular dynamics, pharmacokinetics, and bioactivity prediction. *Journal of Biomolecular Structure and Dynamics*, 1-16.

Ismaya, W. T., Tjandrawinata, R. R., Dijkstra, B. W., Beintema, J. J., Nabila, N., & Rachmawati, H. (2020). Relationship of *Agaricus bisporus* mannose-binding protein to lectins with β-trefoil fold. *Biochemical and Biophysical Research Communications, 527*(4), 1027-1032.

Joshi, R. K. (2016). *Asparagus racemosus* (Shatawari), phytoconstituents and medicinal importance, future source of economy by cultivation in Uttrakhand: A review. *International Journal of Herbal Medicine, 4*(4), 18-21.

Kohn, D. F., & Clifford, C. B. (2002). Biology and diseases of rats. *Laboratory Animal Medicine*, 121-165.

Lakhera, S., Devlal, K., Ghosh, A., Chowdhury, P., & Rana, M. (2022a). Modelling the DFT structural and reactivity study of feverfew and evaluation of its potential antiviral activity against COVID-19 using molecular docking and MD simulations. *Chemical Papers, 76*(5), 2759-2776.

Lakhera, S., Devlal, K., Ghosh, A., & Rana, M. (2021). In silico investigation of phytoconstituents of medicinal herb '*Piper longum*'against SARS-CoV-2 by molecular docking and molecular dynamics analysis. *Results in Chemistry, 3*, 100199.

Lakhera, S., Devlal, K., Rana, M., & Celik, I. (2023a). Study of nonlinear optical responses of phytochemicals of *Clitoria ternatea* by quantum mechanical approach and investigation of their anti-Alzheimer activity with in silico approach. *Structural Chemistry, 34*(2), 439-454.

Lakhera, S., Rana, M., & Devlal, K. (2022b). Theoretical study on spectral and optical properties of essential amino acids: a comparative study. *Optical and Quantum Electronics, 54*(11), 714.

Lakhera, S., Rana, M., & Devlal, K. (2023b). Influence of Adsorption of Gold and Silver Nanoclusters on Structural, Electronic, and Nonlinear optical properties of Pentacene-5, 12-dione: A DFT study. *Optical and Quantum Electronics, 55*(2), 178.

Lakhera, S., Rana, M., & Devlal, K. (2023c). Investigation of nonlinear optical responses of organic derivative of imidazole: imidazole-2-carboxaldehyde. *International Journal of Materials Research, 114*(7-8), 555-563.

Majumdar, S., Gupta, S., Prajapati, S. K., & Krishnamurthy, S. (2021). Neuro-nutraceutical potential of *Asparagus racemosus*: A review. *Neurochemistry International, 145*, 105013.

Mali, S. N., Pandey, A., Bhandare, R. R., & Shaik, A. B. (2022). Identification of hydantoin based Decaprenylphosphoryl-β-d-Ribose Oxidase (DprE1) inhibitors as antimycobacterial agents using computational tools. *Scientific Reports, 12*(1), 16368.

Orr, S. T., Ripp, S. L., Ballard, T. E., Henderson, J. L., Scott, D. O., Obach, R. S., Sun, H., & Kalgutkar, A. S. (2012). Mechanism-based inactivation (MBI) of cytochrome P450 enzymes: structure–activity relationships and discovery strategies to mitigate drug–drug interaction risks. *Journal of Medicinal Chemistry, 55*(11), 4896-4933.

Pappas, P. G. (2013). Cryptococcal infections in non-HIV-infected patients. *Transactions of the American Clinical and Climatological Association, 124*, 61-79.

Pastuch-Gawołek, G., Gillner, D., Król, E., Walczak, K., & Wandzik, I. (2019). Selected nucleos (t) ide-based prescribed drugs and their multi-target activity. *European Journal of Pharmacology, 865*, 172747.

Rashid, F., Javaid, A., Ashfaq, U. A., Sufyan, M., Alshammari, A., Alharbi, M., Nisar, M. A., & Khurshid, M. (2022). Integrating pharmacological and computational approaches for the phytochemical analysis of *Syzygium cumini* and its anti-diabetic potential. *Molecules, 27*(17), 5734.

Remko, M., Boháč, A., & Kováčiková, L. (2011). Molecular structure, pKa, lipophilicity, solubility, absorption, polar surface area, and blood brain barrier penetration of some antiangiogenic agents. *Structural Chemistry, 22*, 635-648.

Remko, M., Swart, M., & Bickelhaupt, F. M. (2006). Theoretical study of structure, pKa, lipophilicity, solubility, absorption, and polar surface area of some centrally acting antihypertensives. *Bioorganic & Medicinal Chemistry, 14*(6), 1715-1728.

Savarino, A. (2007). In-Silico docking of HIV-1 integrase inhibitors reveals a novel drug type acting on an enzyme/DNA reaction intermediate. *Retrovirology, 4*, 1-15.

Sharma, R., & Jaitak, V. (2020). *Asparagus racemosus* (Shatavari) targeting estrogen receptor α:-An in-vitro and in-silico mechanistic study. *Natural Product Research, 34*(11), 1571-1574.

Sherry, D., Pandian, R., & Sayed, Y. (2022). Non-active site mutations in the HIV protease: Diminished drug binding affinity is achieved through modulating the hydrophobic sliding mechanism. *International Journal of Biological Macromolecules, 217*, 27-41.

Sherry, D., Worth, R., Ismail, Z. S., & Sayed, Y. (2021). Cantilever-centric mechanism of cooperative non-active site mutations in HIV protease: Implications for flap dynamics. *Journal of Molecular Graphics and Modelling, 106*, 107931.

Singla, R., & Jaitak, V. (2015). Molecular docking simulation study of phytoestrogens from *Asparagus racemosus* in breast cancer progression. *International Journal of Pharmaceutical Sciences and Research, 6*(1), 172-182.

Sun, X., Zhang, Q., & Al-Hashimi, H. M. (2007). Resolving fast and slow motions in the internal loop containing stem-loop 1 of HIV-1 that are modulated by Mg^{2+} binding: role in the kissing–duplex structural transition. *Nucleic Acids Research, 35*(5), 1698-1713.

Tabe, F. N., Yanou, N. N., Kamdje, A. H. N., & Ntso, A. S. A. (2015). Oxidative Role of HIV/AIDS. Antiretroviral Drugs and Medicinal Plants with Anti-HIV Activity. *Journal of Diseases and Medicinal Plants, 1*(5), 68-75.

Thakur, S., Kaurav, H., & Chaudhary, G. (2021). Shatavari (*Asparagus racemosus*)-the best female reproductive tonic. *International Journal of Research and Review, 8*(5), 73-84.

Varma, M. V., Sateesh, K., & Panchagnula, R. (2005). Functional role of P-glycoprotein in limiting intestinal absorption of drugs: contribution of passive permeability to P-glycoprotein mediated efflux transport. *Molecular Pharmaceutics, 2*(1), 12-21.

Veber, D. F., Johnson, S. R., Cheng, H.-Y., Smith, B. R., Ward, K. W., & Kopple, K. D. (2002). Molecular properties that influence the oral bioavailability of drug candidates. *Journal of Medicinal Chemistry, 45*(12), 2615-2623.

Walsh, B. S., Kesselheim, A. S., & Rome, B. N. (2023). Medicaid Spending on Antiretrovirals From 2007 Through 2019. *Clinical Infectious Diseases, 76*(5), 833-841.

Wang, H., Cohen, A. A., Galimidi, R. P., Gristick, H. B., Jensen, G. J., & Bjorkman, P. J. (2016). Cryo-EM structure of a CD4-bound open HIV-1 envelope trimer reveals structural rearrangements of the gp120 V1V2 loop. *Proceedings of the National Academy of Sciences, 113*(46), E7151-E7158.

Wang, J., Duan, X., Gao, J., Shen, Y., Feng, X., Yu, Z., Tan, X., Liu, S., & Wang, S. (2020). Roles of structure defect, oxygen groups and heteroatom doping on carbon in nonradical oxidation of water contaminants. *Water Research, 185*, 116244.

Wang, J., Kang, X., Kuntz, I. D., & Kollman, P. A. (2005). Hierarchical Database Screenings for HIV-1 Reverse Transcriptase Using a Pharmacophore Model, Rigid Docking, Solvation Docking, and MM− PB/SA. *Journal of Medicinal Chemistry, 48*(7), 2432-2444.

Wang, J., Morin, P., Wang, W., & Kollman, P. A. (2001). Use of MM-PBSA in reproducing the binding free energies to HIV-1 RT of TIBO derivatives and predicting the binding mode to HIV-1 RT of efavirenz by docking and MM-PBSA. *Journal of the American Chemical Society, 123*(22), 5221-5230.

Waring, M. J. (2010). Lipophilicity in drug discovery. *Expert Opinion on Drug Discovery, 5*(3), 235-248.

Weiss, R. (2008). Special anniversary review: twenty-five years of human immunodeficiency virus research: successes and challenges. *Clinical & Experimental Immunology, 152*(2), 201-210.

Zhibin, L., Xia, L., Jiping, Y., Liran, X., & Huijun, G. (2015). Differences in acquired immune deficiency syndrome treatment and evaluation strategies between Chinese and Western Medicine. *Journal of Traditional Chinese Medicine, 35*(6), 718-722.